

Bulk and interfacial properties in colloid-polymer mixtures

R. L. C. Vink,¹ A. Jusufi,² J. Dzubiella,³ and C. N. Likos⁴

¹*Institut für Physik, Johannes-Gutenberg-Universität, Staudinger Weg 7, D-55099 Mainz, Germany*

²*Lehrstuhl für Physikalische Chemie I, Universität Bayreuth, D-95440 Bayreuth, Germany*

³*NSF Center for Theoretical Biological Physics (CTBP), Department of Chemistry and Biochemistry, University of California, San Diego, La Jolla, California 92093-0365, USA*

⁴*Institut für Theoretische Physik II, Heinrich-Heine-Universität Düsseldorf, D-40225 Düsseldorf, Germany*

(Received 10 May 2005; revised manuscript received 26 July 2005; published 8 September 2005)

Large-scale Monte Carlo simulations of a phase-separating colloid-polymer mixture are performed and compared to recent experiments. The approach is based on effective interaction potentials in which the central monomers of self-avoiding polymer chains are used as effective coordinates. By incorporating polymer non-ideality together with soft colloid-polymer repulsion, the predicted binodal is in excellent agreement with recent experiments. In addition, the interfacial tension as well as the capillary length are in quantitative agreement with experimental results obtained at a number of points in the phase-coexistence region, without the use of any fit parameters.

DOI: [10.1103/PhysRevE.72.030401](https://doi.org/10.1103/PhysRevE.72.030401)

PACS number(s): 82.70.Dd, 61.20.Ja

In addition to commercial applications, mixtures of colloids and nonadsorbing polymers are interesting because of their analogy to atomic systems [1]. Much effort has been devoted to understanding the phase behavior of such mixtures. Of particular interest is phase separation, which occurs when the polymer density and diameter of gyration are sufficiently large, leading to the formation of two coexisting phases: one phase lean in colloids and dense in polymers (the colloidal vapor), and one phase dense in colloids and lean in polymers (the colloidal liquid). As was shown by Asakura and Oosawa (AO), phase separation in colloid-polymer mixtures (CPM) is driven by entropy [2]. In the AO description, colloids and polymers are treated as effective spheres, assuming hard-sphere interactions between colloid-colloid and colloid-polymer pairs, while the polymers can interpenetrate freely. A major advance has been the development of a geometry-based density functional for the AO model [3], which has led to a host of intriguing predictions regarding interfacial phenomena within this model [4]. However, when comparing to experiments, quantitative discrepancies arise. An important deficiency of the AO model is that it underestimates the polymer concentration in the colloidal liquid [5,6]. This effect is more pronounced within the free-volume approximation [7], which is also the bulk limit of the density functional of Ref. [3], and it persists when the AO binodals are obtained by means of computer simulations [5,8].

While the colloid-colloid interaction in realistic systems is indeed well described by the hard-sphere potential [9], the colloid-polymer and polymer-polymer interactions are more complex. To circumvent the shortcomings of the AO model, numerous different approaches have been employed, both at the effective [10–13] and at the monomer-resolved [14,15] levels. As a general trend, inclusion of polymer nonideality does improve on the major drawback of the AO model, i.e., it yields higher polymer concentrations in the colloidal liquid [11,13]. A remarkably accurate method to capture polymer nonideality is the “polymer as soft colloid” approach [16]. Here, the polymers’ centers of mass are chosen as effective coordinates while all fluctuating monomers

are canonically integrated out. The sought-for effective potentials are obtained by inverting the correlation functions obtained in Monte Carlo (MC) simulations of self-avoiding random walks (SAW) on a lattice [16–18]. The work of Bolhuis *et al.* [18] has led to an accurate determination of the phase behavior of CPM, demonstrated by direct comparison to experiments [5].

Despite the progress in calculating bulk phase diagrams, accurate predictions of the interfacial tension γ between coexisting phases, a quantity that plays a key role in wetting and interfacial phenomena, remain elusive. Theoretical approaches include the square-gradient approximation [6,19,20], density-functional theory [15,21,22], and simulations [8,12,23]. Experimental data on γ are hard to obtain, mainly due to the very small value of this quantity ($\gamma \sim 1 \mu\text{N/m}$). In several cases [6,19,21], theoretical predictions have been compared to the experimental results of Refs. [24,25]. These comparisons are carried out by plotting the theoretical interfacial tension as a function of the colloid density gap across the binodal, a procedure that tends to obscure the fact that the theoretical and experimental binodals can be in considerable disagreement [6]. Recently, Moncho-Jordà *et al.* [22] used density-functional theory to calculate the interfacial tension employing the interactions of Ref. [5]. However, they adopted a depletion picture, thereby losing the effect of polymer-induced many-body interactions between the colloids. Thus a full two-component treatment of interacting CPM is necessary in order to capture bulk and interfacial behavior quantitatively [22].

In this paper, we demonstrate that simulations of CPM using accurate effective interactions also predict the interfacial properties correctly. A quantitative determination of the latter requires, as an initial step, the calculation of the bulk phase diagram. We consider here the so-called “colloid limit,” where the polymer diameter of gyration σ_G is smaller than the colloid diameter σ_c . Recently, experimental measurements of the interfacial tension and capillary length in the colloid limit became available, to which we can compare

[26]. At the same time, accurate effective interactions for the colloid limit exist, obtained in off-lattice molecular dynamics (MD) simulations of self-avoiding polymer chains [27]. We choose here the central monomer to represent the chain, canonically tracing out the remaining, fluctuating monomers. If the coarse-graining procedure is carried out accurately, the bulk thermodynamics of the mixture should be strictly *independent* of the choice of the effective coordinates [28]. Moreover, for athermal solvents and in the limit of long chains, details of the microscopic monomer-monomer interactions become irrelevant [29]. Thus, the phase behavior

should be independent of whether one adopts for the polymers a lattice, SAW model as done in Ref. [5], or the approach at hand. We will explicitly check whether this requirement is fulfilled.

The colloids are represented by their centers and r denotes the distance between any effective coordinates in the corresponding effective interactions $V_{ij}(r)$, with $i, j = c, p$. The colloid-colloid interaction $V_{cc}(r)$ is given by a hard-sphere potential of diameter σ_c . The colloid-polymer interaction, $V_{cp}(r)$ diverges for $r < \sigma_c/2$ and for larger separations it reads as [27]

$$\beta V_{cp}(r) = \frac{\sqrt{2}\Lambda\sigma_c}{r} \begin{cases} \xi_2 - \ln\left(\frac{2r - \sigma_c}{\sigma_p}\right) - \left(\frac{(2r - \sigma_c)^2}{\sigma_p^2} - 1\right)\left(\xi_1 - \frac{1}{2}\right) & \text{if } \frac{\sigma_c}{2} < r \leq \frac{\sigma_c + \sigma_p}{2}, \\ \xi_2 \frac{1 - \text{erf}[\kappa(2r - \sigma_c)]}{1 - \text{erf}(\kappa\sigma_p)} & \text{if } r > \frac{\sigma_c + \sigma_p}{2}, \end{cases}$$

where σ_p a typical length scale given by $\sigma_p = 0.66\sigma_G$, $\beta = (k_B T)^{-1}$, T the temperature, k_B the Boltzmann constant, $\xi_1 \equiv 1/(1 + 2\kappa^2\sigma_p^2)$, $\xi_2 \equiv (\sqrt{\pi}\xi_1/\kappa\sigma_p)[1 - \text{erf}(\kappa\sigma_p)]\exp(\kappa^2\sigma_p^2)$, and parameters Λ and κ , determined in Ref. [27] by fitting to simulation results. This form was derived in Ref. [27] and pertains to star polymer-colloid interactions for the special case of a star with $f=2$ arms (linear chain in the midpoint representation). The polymer-polymer interaction is given by:

$$\beta V_{pp}(r) = 0.786 \begin{cases} -\ln\left(\frac{r}{\sigma_p}\right) + \frac{1}{2\tau^2\sigma_p^2} & \text{if } r \leq \sigma_p, \\ \frac{1}{2\tau^2\sigma_p^2} \exp[-\tau^2(r^2 - \sigma_p^2)] & \text{if } r > \sigma_p, \end{cases}$$

with τ obtained by requiring that the effective interaction correctly reproduces the second virial coefficient of dilute polymer solutions and resulting in the value $\tau\sigma_p = 1.03$ [27]. To match the experiment of Ref. [26], we consider a mixture of colloids and polymers with the size ratio $q \equiv \sigma_G/\sigma_c = 0.56$. The parameters are $\Lambda = 0.46$, and $\kappa\sigma_p = 0.52715$ [30].

The binodal and the interfacial tension are obtained in the grand canonical ensemble, by MC simulation of a mixture of N_c colloids and N_p polymers, interacting via the above pair potentials. In this ensemble, the temperature, the volume V , and the respective fugacities, z_c and z_p , of colloids and polymers, are fixed, while the number of particles in the system fluctuates. We also introduce the colloid and polymer packing fractions $\eta_{c,p} = (\pi\sigma_{c,G}^3/6)N_{c,p}/V$. Since the interactions are athermal, the temperature plays no role and the phase behavior is set by q and the fugacities. The polymer fugacity is used as a control parameter, analogous to the inverse temperature in fluid-vapor transitions in atomic systems. For a given z_p , we measure the distribution $P(\eta_c)$, defined as the

probability of observing a system with colloid packing fraction η_c . For z_p sufficiently far away from the critical point, phase coexistence is obtained by tuning z_c so that $P(\eta_c)$ becomes bimodal, with two peaks of equal area. The peak at low η_c corresponds to the colloidal vapor phase, the peak at high η_c to the colloidal liquid, and the region in between to phase-separated states [8]. The average peak locations yield the colloid packing fractions in the two phases. The interfacial tension is obtained from the average height of the peaks [8,31]. In order to simulate efficiently, a grand canonical cluster move similar in spirit to Ref. [8] is used, in combination with a reweighting scheme [32].

The resulting phase diagram obtained in the simulation is shown in Fig. 1 and compared to experiments. Note that the

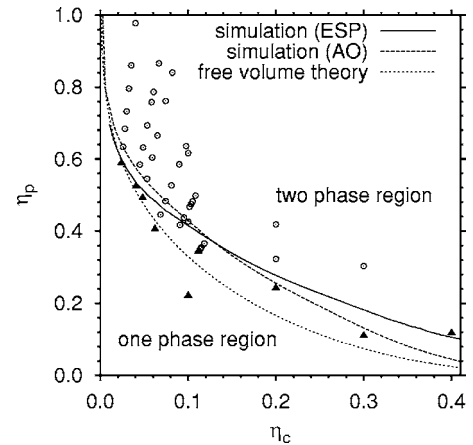


FIG. 1. Colloid-polymer binodals for $q=0.56$ obtained in simulations using two different models (ESP and AO). Open circles are experimental state points at which phase separation was observed; the black triangles are experimental state points at which only one phase was observed. The experimental data were taken from Refs. [26,33]. The free-volume AO binodal is also shown.

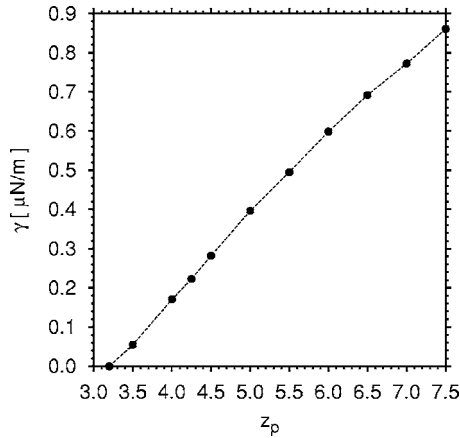


FIG. 2. Interfacial tension γ against the polymer fugacity from our ESP simulations. The line serves to guide the eye.

experiments of Refs. [26,33] pertain to temperatures above the θ point, such that the polymers behave as self-avoiding random walks, thereby justifying the comparison to the present simulation results. The solid curve is the binodal obtained in simulations using the effective soft potentials (ESP) $V_{cp}(r)$ and $V_{pp}(r)$ above. The dashed line shows the binodal of the AO model with $q=0.56$, obtained following the same grand canonical simulation procedure. The free-volume result is also shown. As seen in Fig. 1, ESP interactions give an accurate description of the experimental binodal. Note in particular the significant increase in the polymer density at high colloid density over the AO result. The latter is a consequence of the employed colloid-polymer interaction, which diverges at $\sigma_c/2$. In contrast, in the AO model, the divergence is at $(\sigma_c + \sigma_p)/2$, thereby exceedingly punishing the high polymer concentrations in the colloid-rich phase.

Next, we consider the interfacial tension, and compare it to the recent experiment of Ref. [26]. The colloids are polymethylmethacrylate (PMMA) spheres ($\sigma_c=50$ nm), mixed with a polymer with a diameter of gyration $\sigma_G=28$ nm, and dissolved in decalin at $T=298$ K. In Fig. 2, we show the simulation results of the interfacial tension as a function of z_p . As expected, the tension decreases markedly upon lowering z_p , vanishing at the critical point (the critical polymer fugacity is approximately $z_{p,cr} \approx 3.2$). To enable the comparison to experiment, we show in Fig. 3 several binodal tielines obtained in the simulation. At point X, which is close to the tieline corresponding to $z_p=4.25$, the experimental interfacial tension equals $\gamma=0.16$ to $0.2 \mu\text{N/m}$ [26]. The corresponding interfacial tension in the simulation reads as $\gamma=0.22 \mu\text{N/m}$, which exceeds the experiment by only 10%. In contrast, the interfacial tension obtained at the same state point in a simulation of the AO model is $\gamma=0.07 \mu\text{N/m}$, which underestimates the experiment by over 50%. This is due to subtle differences in the location and range of the critical regions of the two models. More precisely, defining the distance from the critical point as $t \equiv z_p/z_{p,cr} - 1$, we obtain for point X using ESP interactions $t \approx 0.33$, but only $t \approx 0.05$ using the AO model. For the AO model, point X is thus much closer to criticality and hence the interfacial tension is lower. If one calculates the interfacial tension for the

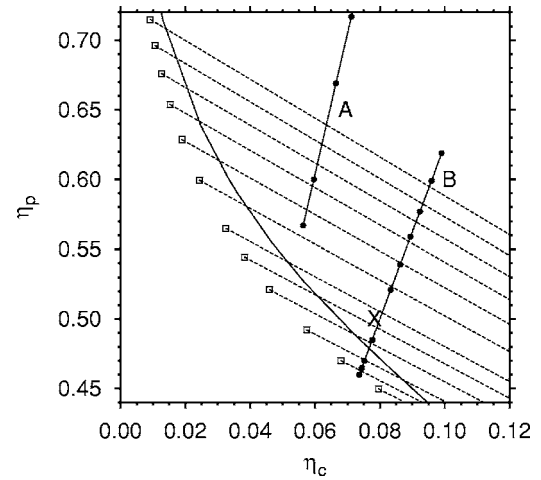


FIG. 3. Close-up of the vapor branch of the binodal. Open squares with tielines (dashed) are binodal points obtained using ESP interactions. The polymer fugacity corresponding to the tielines reads as $z_p=7.5 \rightarrow 7 \rightarrow 6.5 \rightarrow 6 \rightarrow 5.5 \rightarrow 5 \rightarrow 4.5 \rightarrow 4 \rightarrow 3.75 \rightarrow 3.5 \rightarrow 3.45$ (from top to bottom). The solid curve is the binodal of the AO model. The X symbol ($\eta_c=0.076$, $\eta_p=0.50$) marks a state point at which the interfacial tension was measured experimentally [26]. The closed circles on the dilution lines A and B are experimental state points at which the capillary length was measured [26].

AO model using the *free-volume* tieline and square gradient theory at the same state point as in the experiment, the value $\gamma=0.5 \mu\text{N/m}$ is obtained [26]. These discrepancies within the AO model demonstrate the large effect that inaccuracies in the binodals have on γ , as well as ambiguities that arise by comparing interfacial tensions at “rescaled” state points. In our approach, on the contrary, we provide a comparison to the experimentally measured interfacial tension in absolute terms, i.e., at the same state point (η_c, η_p).

Finally, we compare to experimental measurements of the capillary length $l_c = \sqrt{\gamma/(g\Delta\rho)}$, with $g=9.81 \text{ m/s}^2$ the gravitational acceleration, interfacial tension γ , and $\Delta\rho$ the mass

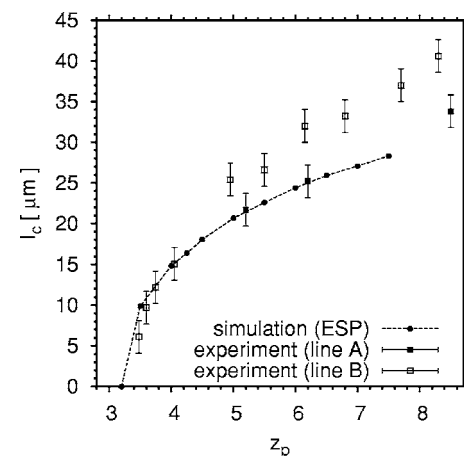


FIG. 4. Capillary length as a function of the polymer fugacity obtained in simulations (ESP), as well as in experiments along dilution lines A and B of Fig. 3 taken from Ref. [26]. The line connecting the simulation data serves to guide the eye.

density difference between the colloidal liquid and vapor phase. For two coexisting phases with colloid- and polymer-packing fraction gaps $\Delta\eta_c$ and $\Delta\eta_p$, respectively, it holds $\Delta\varrho = \Delta\eta_c(\varrho_c - \varrho_d) + \Delta\eta_p m_p/v_p$, with the mass densities $\varrho_c = 1170 \text{ kg/m}^3$ for PMMA and $\varrho_d = 890 \text{ kg/m}^3$ for decalin, $m_p = 3.87 \times 10^{-22} \text{ kg}$ the single polymer mass, and $v_p = \pi\sigma_G^3/6$ the effective single polymer volume [26]. In Fig. 4, we plot the capillary length as obtained in the simulation as function of z_p . The experimental data are also shown, where the conversion to z_p was performed with the aid of Fig. 3 (experimental measurements at $z_p > 7.5$ were converted using linear extrapolation). As $\gamma = g\Delta\varrho l_c^2$ and since $\Delta\varrho$ is given accurately by our approach (as shown by the good agreement with the experimental binodal), the agreement with experiment regarding l_c directly implies agreement with the interfacial tension γ at all considered state points.

In summary, we have demonstrated that the “polymer as soft colloid” approach [16], using accurate effective colloid-polymer and polymer-polymer interactions, not only reproduces the experimental binodal, but also the interfacial ten-

sion and the capillary length. Note that excellent agreement with the experimental binodal was also obtained in Ref. [5], in which the polymer centers of mass were employed as effective coordinates. Both the effective description of Ref. [5], and the one adopted here, thus reproduce the correct thermodynamics, providing a strong confirmation of the power and self-consistency of coarse-graining techniques. We anticipate that a full, two-component calculation of the interfacial tension using the effective interactions of Ref. [5] will also capture the interfacial properties correctly; the latter should be the subject of further investigations. Additional experimental work in measuring interfacial tensions in colloid-polymer mixtures is also highly desirable.

We thank Dirk Aarts for providing experimental data and for helpful discussions. This work was supported by the DFG through the SFB-TR6. Allocation of computer time on the JUMP at the Forschungszentrum Jülich is gratefully acknowledged.

-
- [1] W. Poon, *Science* **304**, 830 (2004).
 [2] S. Asakura and F. Oosawa, *J. Chem. Phys.* **22**, 1255 (1954).
 [3] M. Schmidt *et al.*, *Phys. Rev. Lett.* **85**, 1934 (2000).
 [4] J. M. Brader *et al.*, *Mol. Phys.* **101**, 3349 (2003).
 [5] P. G. Bolhuis *et al.*, *Phys. Rev. Lett.* **89**, 128302 (2002).
 [6] D. G. A. L. Aarts *et al.*, *J. Chem. Phys.* **120**, 1973 (2004).
 [7] H. N. W. Lekkerkerker *et al.*, *Europhys. Lett.* **20**, 559 (1992).
 [8] R. L. C. Vink and J. Horbach, *J. Chem. Phys.* **121**, 3253 (2004).
 [9] A. Imhof and J. K. G. Dhont, *Phys. Rev. Lett.* **75**, 1662 (1995).
 [10] P. B. Warren *et al.*, *Phys. Rev. E* **52**, 5205 (1995).
 [11] M. Schmidt *et al.*, *J. Chem. Phys.* **118**, 1541 (2003).
 [12] R. L. C. Vink and M. Schmidt, *Phys. Rev. E* **71**, 051406 (2005).
 [13] M. Schmidt and M. Fuchs, *J. Chem. Phys.* **117**, 6308 (2002).
 [14] M. Fuchs and K. S. Schweizer, *Phys. Rev. E* **64**, 021514 (2001); *J. Phys.: Condens. Matter* **14**, R239 (2002).
 [15] P. Bryk, *J. Chem. Phys.* **122**, 064902 (2005).
 [16] A. A. Louis *et al.*, *Phys. Rev. Lett.* **85**, 2522 (2000).
 [17] P. G. Bolhuis *et al.*, *J. Chem. Phys.* **114**, 4296 (2001).
 [18] P. G. Bolhuis and A. A. Louis, *Macromolecules* **35**, 1860 (2002).
 [19] J. M. Brader and R. Evans, *Europhys. Lett.* **49**, 678 (2000).
 [20] A. Moncho-Jordà *et al.*, *J. Chem. Phys.* **119**, 12667 (2003).
 [21] J. M. Brader *et al.*, *J. Phys.: Condens. Matter* **14**, L1 (2002).
 [22] A. Moncho-Jordà *et al.*, *J. Phys. Chem. B* **109**, 6640 (2005).
 [23] A. Fortini *et al.*, *Phys. Rev. E* **71**, 051403 (2005).
 [24] E. H. A. de Hoog and H. N. W. Lekkerkerker, *J. Phys. Chem. B* **103**, 5274 (1999).
 [25] D. G. A. L. Aarts *et al.*, *J. Phys.: Condens. Matter* **15**, S245 (2003).
 [26] D. G. A. L. Aarts, *J. Phys. Chem. B* **109**, 7407 (2005).
 [27] A. Jusufi *et al.*, *J. Phys.: Condens. Matter* **13**, 6177 (2001).
 [28] C. N. Likos, *Phys. Rep.* **348**, 267 (2001).
 [29] P. G. de Gennes, *Scaling Concepts in Polymer Physics* (Cornell University Press, Ithaca, N.Y., 1979).
 [30] The value of $\kappa\sigma_p$ quoted in Ref. [27] is slightly higher. Extensive additional MD simulations revealed that a lower value of $\kappa\sigma_p$ yields a better fit to MD data.
 [31] K. Binder, *Phys. Rev. A* **25**, 1699 (1982).
 [32] P. Virnau and M. Müller, *J. Chem. Phys.* **120**, 10925 (2004).
 [33] S. M. Ilett *et al.*, *Phys. Rev. E* **51**, 1344 (1995).